Received: 4 September 2019 | Revised: 21 October 2019 | Accepted: 22 October 2019

DOI: 10.1002/jms.4462

SPECIAL ISSUE - RESEARCH ARTICLE

WILEY Journal of MASS SPECTROMETRY

One electron less or one proton more: how do they differ?

Nick A. van Huizen[1,2] | John L. Holmes[3] | Peter C. Burgers[1]

[1] Department of Neurology, Laboratory of Neuro-Oncology, Erasmus Medical Center, Rotterdam 3015CN, The Netherlands

[2] Department of Surgery, Erasmus Medical Center, Rotterdam 3015CN, The Netherlands

[3] Department of Chemistry and Biological Sciences, University of Ottawa, 10 Marie Curie, Ottawa, Ontario K1N 6N5, Canada

Correspondence
P.C. Burgers, Department of Neurology, Laboratory of Neuro-Oncology, Erasmus Medical Center, Rotterdam 3015 CN, The Netherlands.
Email: p.burgers@erasmusmc.nl

Abstract

From the NIST website and the literature, we have collected the Ionisation Energies (*IE*) of 3,052 and the Proton Affinities (*PA*) of 1,670 compounds. For 614 of these, both the *IE* and *PA* are known; this enables a study of the relationships between these quantities for a wide variety of molecules. From the *IE* and *PA* values, the hydrogen atom affinities (*HA*) of molecular ions $M^{\bullet+}$ may also be assessed. The *PA* may be equated to the heterolytic bond energy of $[MH]^+$ and *HA* to the homolytic bond energy. Plots of *PA* versus *IE* for these substances show (in agreement with earlier studies) that, for many families of molecules, the slope of the ensuing line is less negative than −1, i.e. changes in the *PA* are significantly less than the concomitant opposite changes in *IE*. At one extreme (high *PA*, low *IE*) are the metals, their oxides and hydroxides, which show a slope of close to −1, at the other extreme (low *PA*, high *IE*) are the hydrogen halides, methyl halides and noble gases, which show a slope of ca. −0.3; other molecular categories show intermediate behaviour. One consequence of a slope less negative than −1 is that the changes in ionic enthalpies of the protonated species more closely follow the changes in the enthalpies of the neutral molecules compared with changes in the ion enthalpies of the corresponding radical cations. This is consistent with findings from *ab initio* calculations from the literature that the incoming proton, once attached to the molecule, may retain a significant amount of its charge. These collected data allow a comparison of the thermodynamic stability of protonated molecules in terms of their homolytic or heterolytic bond cleavages. Protonated nitriles are particularly stable by virtue of the very large hydrogen atom affinities of their radical cations.

KEYWORDS

protonated molecules, proton affinity, hydrogen atom affinity, ionisation energy, gas-phase ion chemistry

1 | INTRODUCTION

A great number of mass spectra have been measured, as exemplified by the huge NIST index that contains over 100,000 mass spectra. Most of these spectra have been obtained using electron ionisation. This method requires molecules to be volatile and so places significant limits on its use. Therefore in general, electron ionisation and similar ionisation methods such as photoionisation are restricted to molecules of low molecular weight. Considerable efforts have been made to develop ionisation methods for nonvolatile, thermally labile, and/or

high molecular weight species, such as electrospray ionisation (ESI) and matrix-assisted laser desorption-ionisation (MALDI).

Electron ionisation and photoionisation usually produce radical cations and these processes can be represented as: M ➔ $M^{\bullet+}$ + e^-; the energy *required* for this process is the ionisation energy (*IE*) and the *IE* of a molecule M is given by[1]:

$$IE(M) = \Delta_f H^0(M^{\bullet+}) - \Delta_f H^0(M) \quad (1)$$

From *IE* measurements, the Enthalpies of Formation of $M^{\bullet+}$, $\Delta_f H^0$ ($M^{\bullet+}$), may be assessed. ESI and MALDI usually lead to protonated species and this can be represented as: M + H^+ ➔ $[MH]^+$; the energy *gained* by this process is called the Proton Affinity (*PA*) and so the *PA* of the molecule M is given by[1]:

$$PA(M) = \Delta_f H^0(M) + \Delta_f H^0(H^+) - \Delta_f H^0([MH]^+) \quad (2)$$

where $\Delta_f H^0(H^+)$ is the enthalpy of formation of a proton. From appropriate *PA* measurements, $\Delta_f H^0([MH]^+)$ may be assessed. *IE* and *PA* values are positive numbers.

By inspection, equation (3) follows[2-6]:

$$PA(M) = -IE(M) + IE(H^{\bullet}) + HA(M^{\bullet+}) \quad (3)$$

where *IE*($H^{\bullet}$) is the ionisation energy of a hydrogen atom and *HA*($M^{\bullet+}$) is the hydrogen atom affinity of $M^{\bullet+}$, which can be equated to the homolytic bond dissociation energy of $[MH]^+$, $[MH]^+$ ➔ $M^{\bullet+}$ + $H^{\bullet}$. *PA* can be equated to the heterolytic bond dissociation energy of $[MH]^+$, $[MH]^+$ ➔ M + H^+. (Most of the molecules M studied are closed shell systems; in the case of radicals $M^{\bullet}$, the ionised form is M^+ and the protonated form becomes $[MH]^{\bullet+}$. This will be emphasized when required).

A typical energy diagram of a protonated molecule is shown in Fig. 1 which gives the energy levels for $[MH]^+$, M + H^+ and $M^{\bullet+}$ + $H^{\bullet}$ relative to M + $H^{\bullet}$ (= 0); *PA*, *IE* and *HA* are as indicated, *IE*($H^{\bullet}$) = 1312 kJ/mol. From this figure, Eqn (3) can be derived. Maksić and Vianello[7] point out that because in general *IE*(M) < *IE*($H^{\bullet}$), the *PA* will be larger than *HA*, i.e. proton affinities are often appreciably higher than the average dissociation energy of covalent bonds. This has also been emphasised by Kuck.[8] It is assumed that the original attacking proton is lost as $H^{\bullet}$ or as H^+. For $H^{\bullet}$ atom loss this is not necessarily the case, because the loss of a *different* hydrogen atom may result in a more stable isomeric (distonic) structure,[9] as for example the ion $[CH_3OH_2]^+$ ➔ $[CH_2OH_2]^{\bullet+}$ + $H^{\bullet}$ as opposed to $[CH_3OH_2]^+$ ➔ $[CH_3OH]^{\bullet+}$ + H•.[10] Moreover, the loss of $H^{\bullet}$ may not be the lowest energy process if other direct bond cleavages or rearrangements can take place below the threshold for loss of $H^{\bullet}$. For example, the threshold for the reaction $[CH_3OH_2]^+$ ➔ CH_3^+ + H_2O lies 212 kJ/mol below that for $[CH_3OH]^{\bullet+}$ + $H^{\bullet}$.

Although the ionic species $M^{\bullet+}$ and $[MH]^+$ are distinct, their stabilities will be determined by their ability to accommodate a positive charge. Both electron detachment and proton attachment are adiabatic, that is, electronic and geometrical rearrangements may occur during these processes. The purpose of the present paper is to assess

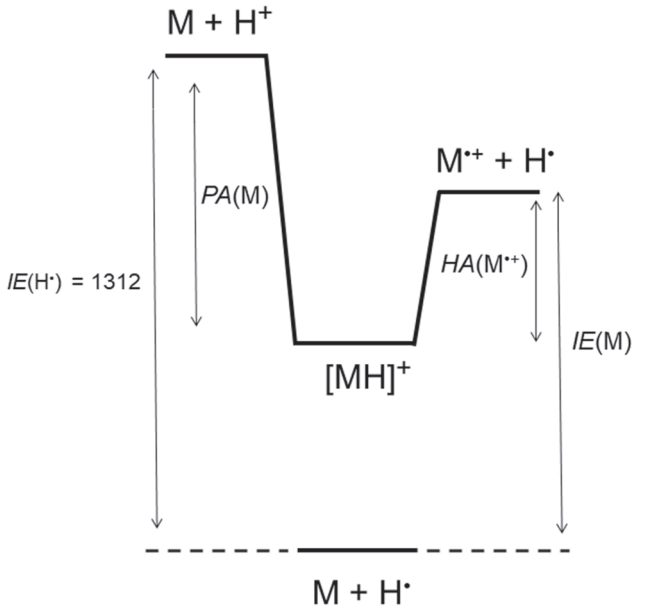

FIGURE 1 Typical energy diagram for the homolytic and heterolytic cleavage of a protonated molecule. The enthalpy for M + $H^{\bullet}$ is set at 0. The ionisation energy of a hydrogen radical is 1312 kJ/mol.

the quantities *IE*, *PA* and *HA* as shown in Eqn (3) for a wide variety of classes of molecules, as has been done previously for other selected categories.[2-6] This we have done by collecting *PA* and *IE* data from the NIST database and calculating *HA* from Eqn (3). Our major objective was to assess the heterolytic (i.e. the *PA*) and homolytic (i.e. the *HA*) bond dissociation energies for a wide variety of protonated molecules, as indicated in Fig. 1, and to evaluate any relationships between *PA* and *HA*. Since a wealth of data is now available, we will provide an overview of the most salient features. Of particular importance for the present study are the stabilisation effects at the charge-bearing site of $M^{\bullet+}$ and $[MH]^+$. That such species can have marked different stabilities was demonstrated recently in a study of protonated $[MH]^+$ and ionised ($M^{\bullet+}$) pyridine-substituted N-heterotriangulenes.[11]

2 | RESULTS AND DISCUSSION

2.1 | Plots of PA against IE

In general, according to Eqn (3), high *PA* values should correspond to low *IE* values and *vice versa*. This is to be expected because a tightly bound electron in a molecule will be hard to remove and at the same time it will also be difficult to covalently attach a proton. However, the value of *HA* will also play a role. Previous work has shown that for many molecule categories, a plot of *PA versus IE* does not yield a line with slope of −1, as expected from Eqn (3) if *HA* does not change, but a significantly less negative slope, i.e. the changes in *PA* are often smaller than the concomitant opposite changes in *IE*. Of particular interest are methyl group substituent effects; such substitutions lead to stabilisation of the charge in both $M^{\bullet+}$ and $[MH]^+$ due to the polarisability of the methyl group.[12] For example, Aue et al[4] observed

that for the series CH_3NH_2, $(CH_3)_2NH$ and $(CH_3)_3N$ a slope of −0.42 ensues, which according to Eqn (3) shows that the *HA* decreases in this order. Henderson et al[13] pointed out that this in turn shows that in these cases the radical cation $M^{\bullet+}$ becomes more stabilised relative to $[MH]^+$ upon methyl substitution, although both $M^{\bullet+}$ and $[MH]^+$ are of the same charge type. These authors conclude that stabilisation of $M^{\bullet+}$ relative to $[MH]^+$ may be expressed in terms of the delocalisation of charge and spin into the methyl groups of $M^{\bullet+}$. The above are substitutions at a charge-bearing site. In contrast, for substitution at the non-charge-bearing site, e.g. CH_3NH_2 ➔ $CH_3CH_2NH_2$ ➔ $(CH_3)_2CHNH_2$➔$(CH_3)_3CNH_2$, a slope of ca. −1 is found, see also Fig. 1 in Ref 4; in this case, the stabilisation is significantly less than in the case of substitution at a charge-bearing site, both in $M^{\bullet+}$ and in $[MH]^+$; for evaluations and discussions of substitutions at charge-bearing and non charge-bearing sites, see Refs.[14-22]

From a literature survey, it appears that the above situation, namely that a plot of *PA versus IE* gives a line with a slope less negative than −1, is the rule rather than the exception. For example Ref. 5 lists the slopes for a variety of classes of compounds and, with the exception of mercaptans (slope = −0.98) and aromatic amines (slope = −1.0), they are all less negative than −1.

To further investigate these matters, we have collected from the NIST website (accessed on February 2017)[23-27] and from the literature the *IE*s of 3,052 and the *PA*s of 1,670 compounds. The data from the NIST website are included in the supplemental (S-1). For 614 substances both the *IE* and *PA* are known and this enables a study of the relationships between these quantities (and of *HA*) for a wide variety of molecule categories, ranging from metal oxides (high *PA*, low *IE*) to the hydrogen halides (low *PA*, high *IE*). The plot of *PA* against *IE* for these 614 compounds is shown in Fig. 2, where the hydrogen radical is as indicated. Also shown in this figure in grey shades are the *HA*s; the darker, the greater the *HA*. In agreement with the argument of Maksić and Vianello,[7] there are only 32 out of 3,052 compounds with an *IE* larger than that for a hydrogen radical (including the noble gases He, Ne, Ar, Kr and the molecules $CF_3C{\equiv}N$, CHF_3 and CO); this reduces to only 18 out of 614 for those compounds for which *both IE* and *PA* have been measured. For the corresponding protonated forms of these molecules, heterolytic cleavage requires less energy than homolytic cleavage, but they are a minority. The dotted line through $H^{\bullet}$ represents the tipping line: to the left *PA* > *HA*, to the right *PA* < *HA*, see also Fig. 1. From Fig. 2 it can be seen that, at best, a weak correlation exists between the *PA* and *IE*. However, as shown in earlier work, much better correlations ensue when categories of molecules are compared.

The *IE* and *PA* histograms are also shown in Fig. 2 (30 bins per axis). The *IE* distribution appears Gaussian but the *PA* distribution is skewed, in that there appears a lack of high *PA* values; thus high *PA* values are less frequent than low *IE* values. (This is also apparent from the histogram of all 1,670 collected *PA* values, although in that case it could be argued that such high *PA* values have simply not been measured.)

We will first discuss some cases on the extremities of the plot in Fig. 2, namely, compounds with high *PA* and low *IE* on the one hand, and those with low *PA* and high *IE* on the other.

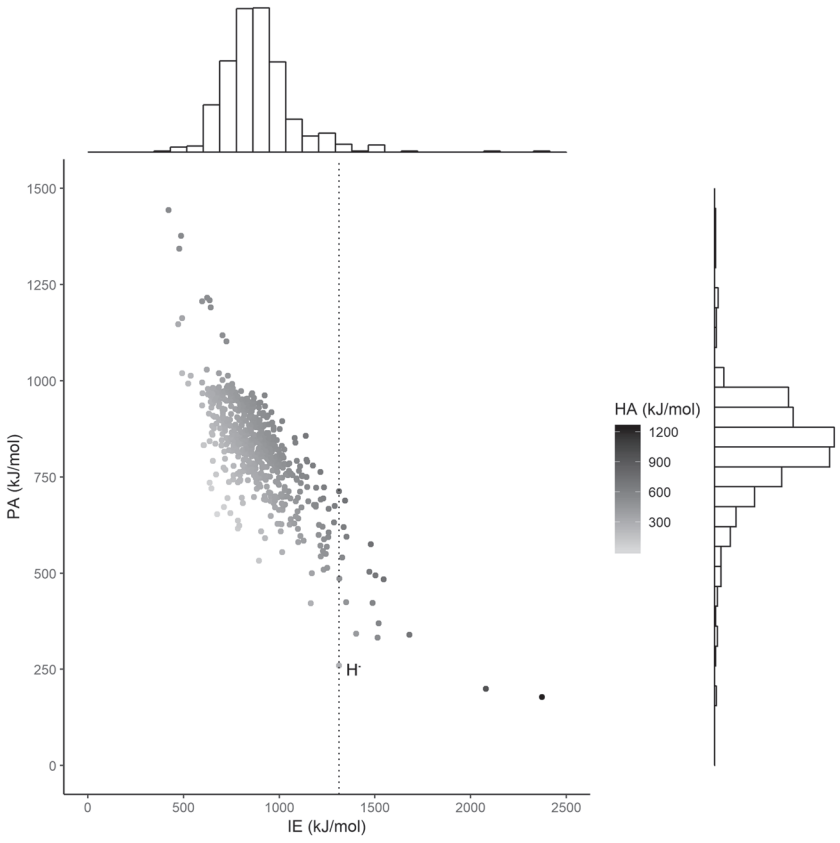

FIGURE 2 Plot of the *PA* versus the *IE* for 614 compounds. The shade of the data points indicates the magnitude of *HA* as indicated. In the margins opposing the x- and y-axis, a histogram of *IE* and *PA* is plotted, respectively. The x- and y-axis are divided in 30 bins to create the histograms. Vertical dashed line indicates *IE*($H^{\bullet}$).

It appears that the metal oxides and hydroxides (Cs_2O, K_2O, Na_2O, Li_2O, SrO, CaO, CsOH, KOH and FeO) have the largest measured *PA*s *and* lowest measured *IE*s. A plot of *PA* against *IE* is given in Fig. 3a (in the following graphs, the *PA* and *IE* axes have the same scale). The data point for SrOH is clearly an outlier, probably because Sr in SrOH has a valency of +1; thus this data point may belong to a different family of species. It is clear that the slope of the line is close to −1 (−1.17 ± 0.05 [95% confidence interval]). In such a situation, *HA* would remain relatively constant as indeed is the case, see Fig. 3b in which *HA* is plotted against *PA*. At this point it is worth noting that such *PA* versus *IE* curves as shown in Fig. 3a have predictive value: for example, the *IE* for NaOH is unknown, but can be estimated from its known *PA*, 1072 kJ/mol and from Fig. 3a, *IE* (NaOH) = 737 kJ/mol. Conversely, the measured *IE* of Rb_2O is 447 kJ/mol, leading to an estimated *PA* of 1410 kJ/mol. For MgO the NIST data base lists two values for its *IE*, 845 and 936 kJ/mol, but the former is more in keeping with that (808 kJ/mol) estimated from its *PA* (988 kJ/mol).

At slightly lower *IE*s are the metal atoms, see Fig. 4,[28] and although the data are somewhat scattered, the slope here, too, is close to −1 (−1.18 ± 0.09 [95% confidence interval]).

At very high *IE* and low *PA* values are the noble gases. As can be seen from Fig. 5a, a plot of *PA versus IE* gives a shallow line, with a slope of only −0.27. For such a shallow line, the *HA* affinity decreases rapidly with *PA*, see Fig. 5b. This figure also shows that the heterolytic bond dissociation energy of $[HeH]^+$ is exceedingly large, 1239 kJ/mol and this has been reported previously.[8] The noble gases represent an extreme case, but other classes of compounds also behave like the noble gases in this respect, such as the hydrogen halides (HX), methyl halides (CH_3X, X = F, Cl, Br, I) and the hydrogen chalcogenides, H_2Y (Y = O, S, Se, Te) for which the *PA* versus *IE* curves have slopes of −0.26, −0.32 and −0.11 respectively, see below.

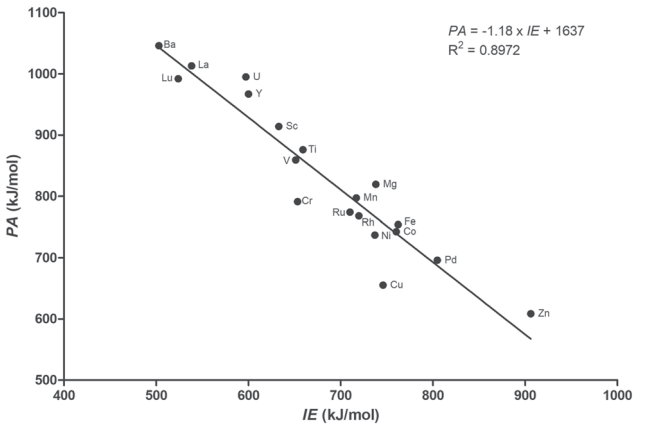

FIGURE 4 *PA* versus *IE* plot for the metals. *PA* (Ba) = 1046 kJ/mol, taken from Ref.[28]

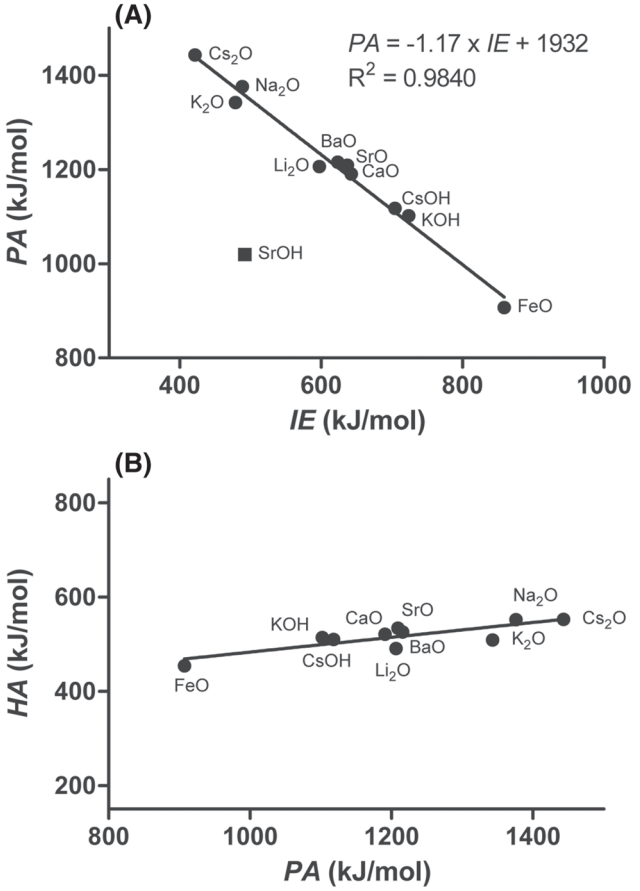

FIGURE 3 (A) *PA* versus *IE* plot for the metal oxides and metal hydroxides. (B) Plot of *HA* versus *PA*.

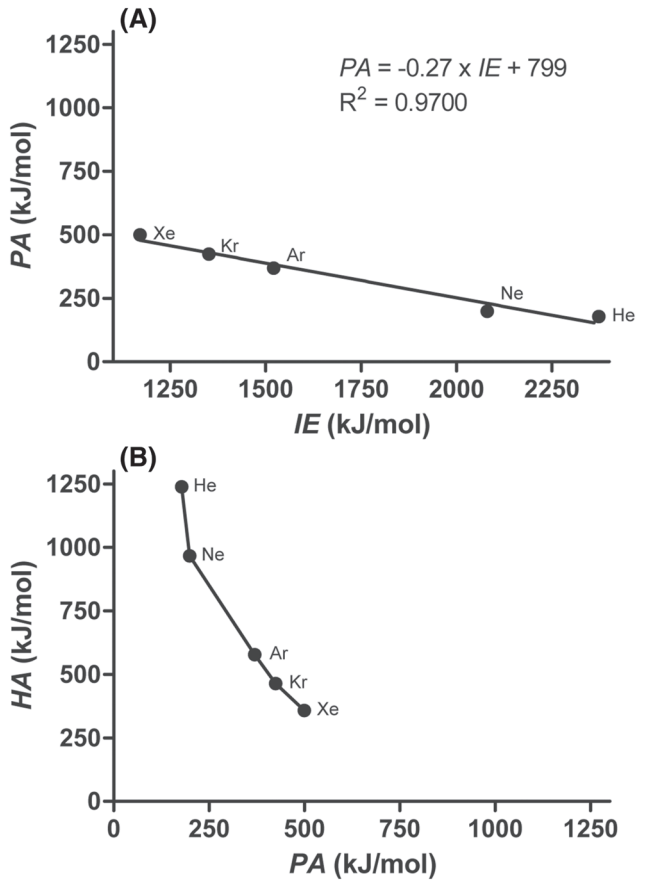

FIGURE 5 (A) *PA* versus *IE* plot for noble gases. (B) *HA* versus *PA* for noble gases.

From these extreme situations, a simple (but possibly incorrect and/or incomplete, see below) interpretation may ensue. For molecules M having large *PA*s, transfer of H^+ to M may be more or less complete and the protonated molecule can be represented as M^+-H. In that case, any stabilisation in M^+-H may also be present to about the same extent in $M^{\bullet+}$ and so a slope of −1 will ensue. With respect to the results of the above metals (Fig. 4), we note that calculations by Galbraith et al[29] on protonated metal atoms $[MetH]^+$ (Met = Sc, Ti, V, Cr, MN, Co, Ni, Cu and Zn) have shown the charge on $[MetH]^+$ to be 90% on the metal atom and so $[MetH]^+$ is better represented as Met^+-H, rather than the protio structure Met-H^+. By contrast, for molecules of low *PA*, $[MH]^+$ may well be better represented as M-H^+ where the nature of M, as far as the *PA* goes, is not as important as for M^+-H, hence resulting in a shallow *PA* versus *IE* line.

It appears, also from the literature, that for intermediate *PA* and *IE* values, many different values for the slopes may be obtained. As mentioned above, the methyl substituent is the archetype for studying charge stabilisation effects. A charge (positive or negative) will be stabilised by a methyl substituent due to polarisation of the methyl group.[12] Indeed, it is found that methyl substitution always leads to an increase in *PA* (and a decrease in *IE*). Celebrated cases of this effect are the amines and phosphines, XH_3, CH_3XH_2, $(CH_3)_2XH$ and $(CH_3)_3X$ (X = N, P) and we present here the NIST data to highlight the marked difference in behaviour of these two subsets of molecules. For the amines, a plot of *PA* versus *IE* yields a line with a slope of −0.44,[2] but for the phosphines a slope of −1.00 ensues.[30] Thus, for the nitrogen series the *PA* increases from 845 kJ/mol to 948 kJ/mol (an increase of 103 kJ/mol) whereas for the phosphorous analogues, the *PA* increases by a significantly larger amount (174 kJ/mol, from 785 kJ/mol to 959 kJ/mol). Thus, *PA* (PH_3) < *PA* (NH_3) but *PA*($P(CH_3)_3$) > *PA*($N(CH_3)_3$). The respective slopes of −0.44 and −1.00 indicate that for the amines, *HA* decreases with *PA*, but for the phosphines, *HA* remains virtually constant, see also Fig. 6 in which is plotted *HA* versus *PA* for XH_3, CH_3XH_2, $(CH_3)_2XH$ and $(CH_3)_3X$. Two rationales may be provided for this marked difference in behaviour. Valadbeigi and Gal[31] interpret the *PA*s of these (and other) compounds in terms of dipole (μ) and polarisability (α) contributions. Since the dipole moment

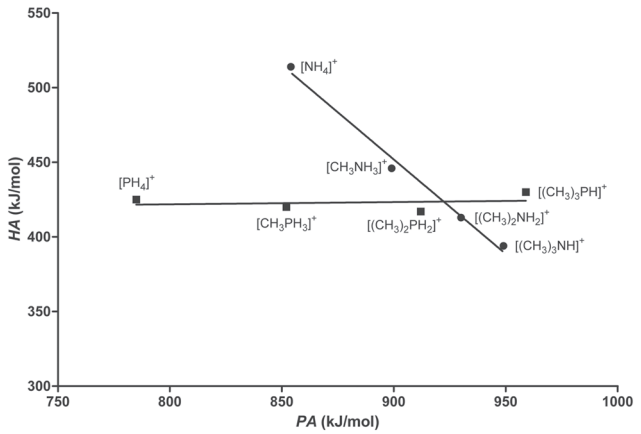

FIGURE 6 Plot of *HA* versus *PA* for ammonia and phosphine and their methyl derivatives.

decreases in the order NH_3 > CH_3NH_2 > $(CH_3)_2NH$ > $(CH_3)_3N$, but increases in the order PH_3 < CH_3PH_2 < $(CH_3)_2PH$ ≈ $(CH_3)_3P$, the dipole contribution to the *PA* becomes less for the amines but would increase for the phosphorous analogues in the above order. (For a more detailed discussion of the dipole moments of these compounds and of their relation with NMR chemical shifts, we refer to the electron momentum spectroscopy study of Rolke and Brion.[32]) Hence, the *PA* for the phosphorous series rises more rapidly with sequential methyl substitution than for the nitrogen analogues and the *HA*s remain virtually constant. Such an effect was also considered in an early paper by Staley and Beauchamp[30] who offer an interpretation in terms of different hybridisation effects upon methyl substitution. A different approach was introduced by Shirley et al.[33] In this approach the proton attachment reaction can be split into two hypothetical steps.[33,34] In the first, the proton attaches itself to an atom (for example nitrogen) without flow of charge in the molecular framework; shifts in energy of this 'reaction' are due to differences in the electron density about the nitrogen in the ground state and are inductive effects. In the second (hypothetical) step, the excess charge is distributed over the whole molecule to minimise Coulombic repulsion (relaxation or polarisation effects). Several groups agree that differences in relaxation energies (rather than differences in inductive effects) are important in protonation (and in core ionisation) processes,[35,36] and that changes in *IE* *also* reflect changes in inductive effects.[34] Thus, it may well be that in the case of the phosphines, inductive effects are more important than in the case of the amines.

Another approach yet may lie in the following. In a study of the above molecules, Reed[37] introduced the concept of 'atomic charging energy', the energy required to bring each atom to the charge it would carry in the product molecules and found this to be a significant part of the proton affinity. He also found that upon protonation, charge transfer is not complete and that different bases transfer different amount of charges. Wiberg et al. find that for protonation of NH_3, all the added positive charge (and a little more) appears at the hydrogens[38]; they conclude that in general hydrogens at the periphery of the ion should be capable of stabilising an ion. In this respect it is of interest to note that early work by Slee and Bader[39] showed that the *PA*s of substituted aldehydes are inversely proportional to the charge of the 'proton' in the protonated carbonyl groups. This behaviour was later also found for other small molecules.[40,41] In particular, Luis López et al[42] find, for nitriles, a linear correlation between the *PA* and the electron population gained by the attacking proton and that the proton keeps a very positive charge (always greater than +0.62 au) when attached to the nitrile; the latter is more in keeping with the structure H^+-N≡C-R (M-H^+) than with the H-N^+≡C-R and H-N=C^+-R (M^+-H) ones. In the same vein, Hughes and Popelier[43] found that in protonated amino acids, the attacking proton keeps about 50% of its charge. We are currently investigating whether such effects also apply to the amine and phosphine (and also to other) series.

By evaluating many categories of molecules, we could not find any relation between the slope of the line and the *PA* or *IE*. However, a relationship within the periodic system does appear to exist. As

TABLE 1 Slopes of methyl group substitution *PA versus IE* curves for (sequential) methyl substitution in the parent compound. R^2 values in parentheses

CH_4 −0.64 (0.920)	NH_3 −0.44 (0.997)	H_2O −0.40 (0.995)	HF −0.34
	PH_3 −1.00 (0.994)	H_2S −0.73 (0.995)	HCl −0.62
			HBr −0.73
			HI −0.78

mentioned above, a methyl substituent always stabilises a charge and we have collected such data for CH_4, NH_3 (and PH_3), H_2O (and H_2S), HF (and HCl, HBr, HI) and present the slopes of the *PA* versus *IE* curves in Table 1. The R^2 values (in parentheses) are also listed except for the halides for which only two data points exist. It can be seen that the slope increases from left to right and from top to bottom. Thus for example for HF, the increase in *PA* for CH_3F is only ca. ⅓ of the decrease in *IE* and so forth. We are currently investigating the origin of these effects by *ab initio* charge distribution calculations.

2.2 | *PA* and *HA*

It has been shown above (and also in the literature) that for many categories of gaseous species an inverse relationship exists between the *PA* (the heterolytic bond energy) of its protonated form and the *HA* (the homolytic bond energy) of its ionised form. This happens when the slope of the *PA* versus *IE* line is less negative than −1, and is frequently the case. Thus, the stronger the heterolytic bond in $[MH]^+$, the weaker the homolytic bond will be and *vice versa*. This may be referred to as a stockholder principle along the lines of Maksić and Vianello,[7] i.e. the more investment in *PA*, the more profit in *HA*.

As has been pointed out previously,[8] the *HA* is a significant property of a radical cation $M^{\bullet+}$. *HA* data allow the estimation of the driving force for $H^\bullet$ abstraction by an ionised functional group from a neutral $H^\bullet$ donor, for example, a C-H bond. It appears that many radical cation centres are very strong $H^\bullet$ acceptors and therefore many intramolecular (and intermolecular) transfers of a hydrogen atom from an aliphatic chain to a cation centre have little energy requirements or can even be exothermic[8] making rearrangement reactions via distonic ions possible, for example in the McLafferty rearrangement. Thus from the NIST compilation, the *HA* of the 2-pentanone radical cation is 426 kJ/mol, whereas the C-H bond dissociation energy of e.g. ethane is 420 kJ/mol. Hence, the thermochemistry of isomerisation of radical cations by $H^\bullet$ (as well as H^+) transfers can be estimated from thermochemical data.[8] Kuck also concludes that radical cations of aliphatic nitriles have very high *HA*s and we agree: the largest *HA*s are for (in that order): $He^{\bullet+}$, $Ne^{\bullet+}$, $SF_6{}^{\bullet+}$, $CF_3C{\equiv}N^{\bullet+}$, $HF^{\bullet+}$, and $HC{\equiv}N^{\bullet+}$ with $CH_3C{\equiv}N^{\bullet+}$ and $CH_3CH_2C{\equiv}N^{\bullet+}$ on position 15 and 17 respectively (out of 614). When we order our data according to the lowest of either *PA* or *HA*, i.e. according to stability, we find at the top $[HC{\equiv}NH]^+$, and $[CH_3C{\equiv}NH]^+$ and $[CH_3CH_2C{\equiv}NH]^+$ at position 7 and 8, respectively. Thus, protonated nitriles are among the most stable protonated molecules.

2.3 | Ionic heats of formation

From the above, it appears that plots of *PA* versus *IE* are very often lines with a slope less negative than −1. This indicates that *HA* decreases with increasing *PA*,[4] but it also means that, for a given category of molecules, the changes in ionic enthalpies of the protonated species more closely follow the changes in the enthalpies of the neutral molecules, compared with changes in the ion enthalpies of the

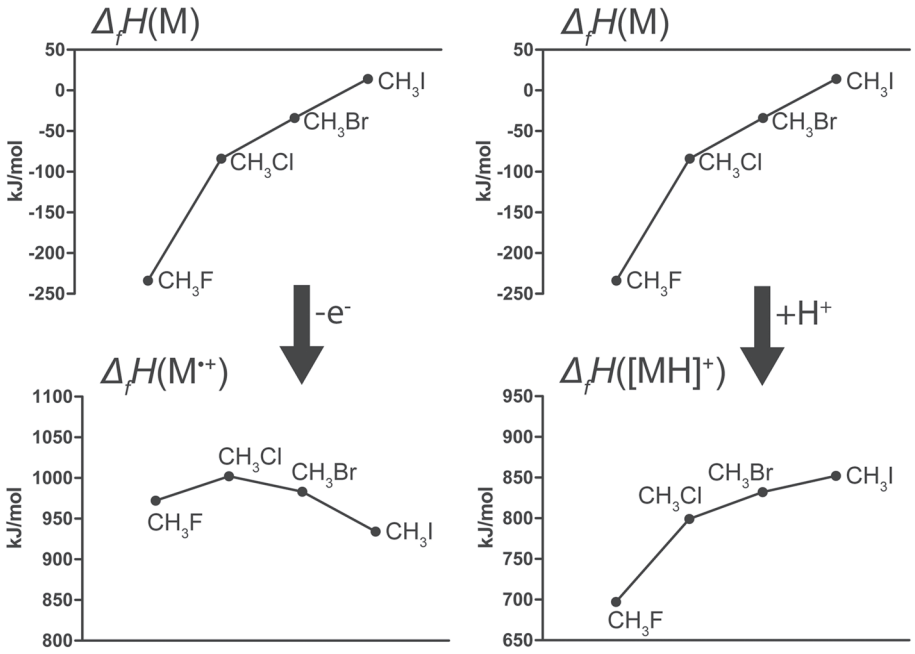

FIGURE 7 Heats of formation of the neutral methyl halides, top; of the radical cations, bottom, left; of the protonated species, bottom, right.

radical cations.[34] This is consistent with findings from *ab initio* calculations, see above, that the incoming proton, once attached to the molecule, may retain a significant amount of its charge.[39-43] This effect is discussed here for the methyl halides CH_3X (X = F, Cl, Br, I), but the phenomenon is general. The *PA* versus *IE* line of the methyl halides has a slope of −0.32. In Fig. 7 are shown the heats of formation of neutral CH_3X (top) and the heats of formation of $[CH_3X]^{+\bullet}$ and $[CH_3XH]^+$ (below) on the same scale. We can see that for the radical cation there is considerable charge stabilisation due to charge dispersal when the size of the halogen atom increases. However, this effect is much less for the protonated species and the heats of formation now more closely follow those of the neutral species. (This effect also occurs markedly for the halide *radical atoms* $X^\bullet$ and for the hydrogen halides HX.) This phenomenon occurs whenever the *PA* versus *IE* slope is less negative than −1, which is usually the case. This means that charge stabilisation effects can best be studied by a comparison of the heats of formation of $M^{\bullet+}$ rather than of $[MH]^+$. An extreme example is provided by the hydrogen chalcogenides, H_2X (X = O, S, Se, Te). Here the slope of the *PA versus IE* curve is only −0.11 and thus the heats of formation of $[H_3X]^+$ almost exactly follow those of H_2X. Also, *HA* (the homolytic bond dissociation energy, kJ/mol) falls rapidly in the order H_3O^+ (597) > H_3S^+ (402) > H_3Se^+ (350) > H_3Te^+ (306). We propose that these observations deserve additional study, for example it would be of interest to see whether H_2Po, for which *IE* = 830 kJ/mol and for which the *PA* and thus *HA* is unknown, follows this trend. One possible rationalisation might be that for both $[H_3X]^+$ and H_2X the charges on the hydrogens are similarly large, but in the absence of *ab initio* calculations this must remain speculative.

At this point it is appropriate to discuss the various possibilities of the magnitude of the *PA* versus *IE* slope in terms of stabilisation relative to $M^{\bullet+}$. We list the following possibilities in Table 2.

Most of the molecular categories fall in the range $-1 < s < 0$. We have not encountered $s \geq 0$, a result that would imply no charge stabilisation and even destabilisation in $[MH]^+$ relative to M. Of interest could be cases where $s < -1$. In such cases $[MH]^+$ would be more stabilised than $M^{\bullet+}$. This may be the case to a minor extent in the metals and metal oxides for which slopes of −1.18 ± 0.09 (95% confidence interval) and −1.17 ± 0.05 (95% confidence interval) were found. For example for the protonated transition metal atoms, the structure M^{2+}-H^- may contribute to its stability, which is not possible in $M^{(\bullet)+}$.

TABLE 2 Possible slopes of *PA* versus *IE* line and implications for stabilisation of family of ions $[MH]^+$

Slope (s) of *PA* versus *IE* line	Stabilisation
s = −1	$[MH]^+ = M^{\bullet+}$
−1 < s < 0	$[MH]^+ < M^{\bullet+}$
s = 0	$[MH]^+ < M^{\bullet+}$and $[MH]^+ = M$
s > 0	$[MH]^+ < M^{\bullet+}$and $[MH]^+ < M$
s < −1	$[MH]^+ > M^{\bullet+}$

2.4 | Summary

A data base (NIST) mining study of the heterolytic (= proton affinity) and homolytic (= hydrogen atom affinity) bond strengths of 614 protonated species $[MH]^+$ reveals that for many classes of closely related compounds an inverse relationship exists between these two quantities. This follows from the observation that the slopes of the lines for the proton affinity (*PA*) versus ionisation energy (*IE*) plots are very often less negative than −1, as also found previously. As a consequence, for many categories of molecules, changes in ion enthalpies of the protonated molecules follow more closely the changes in neutral enthalpies, compared with changes in enthalpies of the corresponding radical cations, formed by electron detachment. This is consistent with findings from *ab initio* calculations from the literature, that the incoming proton, once attached to the molecule, *may retain a significant amount of its charge*. An extreme example of this phenomenon is provided by the hydrogen chalcogenides, H_2X (X = O, S, Se, Te). Here the slope of the *PA versus IE* curve is only −0.11 and thus the heats of formation of $[H_3X]^+$ almost exactly follow those of H_2X. These findings deserve additional study.

ORCID

Peter C. Burgers https://orcid.org/0000-0003-3418-8438

REFERENCES

1. Holmes JL, Aubrey C, Mayer PM. *Assigning Structures to Ions in Mass Spectrometry*. London: CRC press; 2007.
2. Dekock RL, Barbachyn MR. Proton Affinity, Ionization-Energy, and the Nature of Frontier Orbital Electron-Density. *J Am Chem Soc*. 1979;101(22):6516-6519.
3. Choi SC, Boyd RJ. Equilibrium Structures, Proton Affinities, and Ionization-Potentials of the Fluoroacetones. *Can J Chem-Revue Canadienne De Chimie*. 1985;63(4):836-842.
4. Aue DH, Webb HM, Bowers MT. Quantitative Relative Gas-Phase Basicities of Alkykamines. Correlation with Solution Basicity. *J Am Chem Soc*. 1972;94(13):4726-4728.
5. Lias SG et al. Gas-Phase Ion and Neutral Thermochemistry. *J Phys Chem Ref Data Monogr*. 1988;17:1-861.
6. Campbell S, Beauchamp JL, Rempe M, Lichtenberger DL. Correlations of Lone Pair Ionization Energies with Proton Affinities of Amino-Acids and Related-Compounds - Site Specificity of Protonation. *Int J Mass Spectrom Ion Process*. 1992;117(1-3):83-99.
7. Maksic ZB, Vianello R. Quest for the origin of basicity: Initial vs final state effect in neutral nitrogen bases. *J Phys Chem B*. 2002;106(2):419-430.
8. Kuck D. Structures and properties of gas phase organic ions. In: Nibbering NMM, ed. *The Encyclopedia of mass spectrometry*. Vol.4, Topic B01 Amsterdam: Elsevier; 2005:97-115.
9. Bouma WJ, Nobes RH, Radom L. The Methylenoxonium Radical Cation ($CH_2OH_2^{+\cdot}$) - a Surprisingly Stable Isomer of the Methanol Radical Cation. *J Am Chem Soc*. 1982;104(10):2929-2930.
10. Holmes JL, Lossing FP, Terlouw JK, Burgers PC. The Radical Cation $[CH_2OH_2]^{+\cdot}$ And Related Stable Gas-Phase Ion-Dipole Complexes. *J Am Chem Soc*. 1982;104(10):2931-2932.
11. Hitzenberger JF, Dral PO, Meinhardt U, et al. Stability of Odd- Versus Even-Electron Gas-Phase (Quasi)Molecular Ions Derived from

Pyridine-Substituted N-Heterotriangulenes. *ChemPlusChem*. 2017; 82(2):204-211.

12. Brauman JL, Blair LK. Gas-Phase acidities of Alcohols. *J Am Chem Soc*. 1970;92(19):5986-5992.
13. Henderson WG, Taagepera M, Holtz D, McIver RT Jr, Beauchamp JL, Taft RW. Methyl Substituent Effects in Protonated Aliphatic Amines and Their Radical Cations. *J Am Chem Soc*. 1972;92:4728-4729.
14. Holmes JL, Lossing FP. Towards a General Scheme for Estimating the Heats of Formation of Organic Ions in the Gas-Phase 2. The Effect of Substitution at Charge-Bearing Sites. *Can J Chem-Revue Canadienne De Chimie*. 1982;60(18):2365-2371.
15. Lossing FP, Holmes JL. Stabilization Energy and Ion Size in Carbocations in the Gas-Phase. *J Am Chem Soc*. 1984;106(23):6917-6920.
16. Aubry C, Holmes JL. Correlating thermochemical data for gas-phase ion chemistry. *Int J Mass Spectrom*. 2000;200(1-3):277-284.
17. Holmes JL, Aubry C. Neutral and Ion Thermochemistry: Its Present Status and Significance. *Mass Spectrom Rev*. 2009;28(4):694-700.
18. Holmes JL, Aubry C. Methods for critically assessing old and for estimating new organic gas-phase neutral and ion thermochemical data. A user's guide. *Int Rev Phys Chem*. 2014;33(2):209-228.
19. Leach S. Size effects on cation heats of formation. I. Methyl substitutions in nitrogenous compounds. *Chem Phys*. 2012;392(1):170-179.
20. Leach S. Size Effects on Cation Heats of Formation. II. Methyl Substitutions in Oxygen Compounds. *J Phys Chem B*. 2013;117(39): 10058-10067.
21. Leach S. Size Effects on Cation Heats of Formation. III. Methyl and Ethyl Substitutions in Group IV XH_4, X = C, Si, Ge, Sn, Pb. *J Phys Chem B*. 2014;118(48):11417-11431.
22. Leach S. Size effects on cation heats of formation. IV. Methyl and ethyl substitutions in methyl, methylene, acetylene and ethene. *Mol Phys*. 2015;113(15-16):2302-2319.
23. Afeefy HY, Liebman JF, Stein SE. "Neutral Thermochemical Data", NIST Chemistry WebBook, NIST Standard Reference Database Number 69, Eds. P.J. Linstrom and W.G. Mallard, National Institute of Standards and Technology, Gaithersburg MD, 20899.
24. Hunter EP, Lias SG. "Proton Affinity Evaluation", NIST Chemistry WebBook, NIST Standard Reference Database Number 69, Eds. P.J. Linstrom and W.G. Mallard, National Institute of Standards and Technology, Gaithersburg MD, 20899.
25. Lias SG. "Ionization Energy Evaluation", NIST Chemistry WebBook, NIST Standard Reference Database Number 69, Eds. P.J. Linstrom and W.G. Mallard, National Institute of Standards and Technology, Gaithersburg MD, 20899.
26. Meot-mer MM. "Ion Thermochemistry Data", NIST Chemistry WebBook, NIST Standard Reference Database Number 69, Eds. P.J. Linstrom and W.G. Mallard, National Institute of Standards and Technology, Gaithersburg MD, 20899.
27. Rosenstock HM, Draxl K, Steiner BW. Herron JT. "Ion Energetics Data", NIST Chemistry WebBook, NIST Standard Reference Database Number 69, Eds. P.J. Linstrom and W.G. Mallard, National Institute of Standards and Technology, Gaithersburg MD, 20899.
28. Armentrout PB, Beauchamp JL. Experimental and Theoretical-Studies of the Reaction $Ba^+(D_2,D)BaD^+$ - Sequential Impulse Model for Endothermic Reactions. *Chem Phys*. 1980;48(3):315-320.
29. Galbraith JM, Shurki A, Shaik S. A valence bond study of the bonding in first row transition metal hydride cations: What energetic role does covalency play? *J Phys Chem B*. 2000;104(6):1262-1270.
30. Staley RH, Beauchamp JL. Basicities and Ion-Molecule Reactions of the Methylphosphines in the Gas Phase by Ion Cyclotron Resonance Spectroscopy. *J Am Chem Soc*. 1974;96(20):6252-6260.
31. Valadbeigi Y, Gal JF. Directionality of Cation/Molecule Bonding in Lewis Bases Containing the Carbonyl Group. *J Phys Chem B*. 2017; 121(36):6810-6822.
32. Rolke J, Brion CE. Studies of the electron density in the highest occupied molecular orbitals of PH_3, PF_3 and P $(CH_3)_3$ by electron momentum spectroscopy and Hartree-Fock, MRSD-CI and DFT calculations. *Chem Phys*. 1996;207(1):173-192.
33. Martin RL, Shirley DA. The Relation of Core-Level Binding Energy Shifts to Proton Affinity and Lewis Basicity. *J Am Chem Soc*. 1974;96 (17):5299-5304.
34. Holmes JL, van Huizen NA, Burgers PC. Proton affinities and ion enthalpies. *Eur J Mass Spectrom*. 2017;23(6):341-350.
35. Davis DW, Rabalais JW. Model for Proton Affinities and Inner-Shell Electron Binding Energies Based on the Hellmann-Feynman Theorem. *J Am Chem Soc*. 1974;96(17):5305-5311.
36. Nordfors D, Martensson N, Agren H. A Thermochemical Study of Relations between Proton Affinities and Core Electron-Binding Energies. *J Electron Spectros Relat Phenom*. 1990;53(3):129-139.
37. Reed JL. Electronegativity - Proton Affinity. *J Phys Chem*. 1994;98(41): 10477-10483.
38. Wiberg KB, Schleyer PV, Streitwieser A. The role of hydrogens in stabilizing organic ions. *Can J Chem-Revue Canadienne De Chimie*. 1996;74(6):892-900.
39. Slee T, Bader RFW. Properties of Atoms in Molecules - Protonation at Carbonyl Oxygen. *J Mol Struct-Theochem*. 1992;87:173-188.
40. Alkorta I, Picazo O. Influence of protonation on the properties derived from electron density. *Arkivoc*. 2005;9:305-320.
41. Grana AM, Mosquera RA. Effect of protonation on the atomic and bond properties of the carbonyl group in aldehydes and ketones. *Chem Phys*. 1999;243(1-2):17-26.
42. Lopez JL, Grana AM, Mosquera RA. Electron Density Analysis on the Protonation of Nitriles. *J Phys Chem B*. 2009;113(11):2652-2657.
43. Hughes TJ, Popelier PLA. Where does charge reside in amino acids? The effect of side-chain protonation state on the atomic charges of Asp, Glu, Lys, His and Arg. *Comput Theor Chem*. 2015;1053:298-304.

SUPPORTING INFORMATION

Additional supporting information may be found online in the Supporting Information section at the end of the article.

How to cite this article: van Huizen NA, Holmes JL, Burgers PC. One electron less or one proton more: how do they differ?. *J Mass Spectrom*. 2019;1–8. https://doi.org/10.1002/jms.4462